On the Existence of Transition-Metal Fullerides: Deposition and Characterization of Ti_xC_{60}

L. Norin and U. Jansson*

Uppsala University, Ångström Laboratory, Inorganic Chemistry, Box 538, S-751 21 Uppsala, Sweden

C. Dyer

Renishaw, Old Town, Wotton-under-Edge, Gloucestershire, GL 12 7DH, United Kingdom

P. Jacobsson

Department of Physics, Chalmers, S-412 96 Göteborg, Sweden

S. McGinnis

Intevac, VSD, 3550 Bassett Street, Santa Clara, California 95054

Received December 4, 1997. Revised Manuscript Received February 17, 1998

Titanium fulleride films (Ti_xC_{60}) were prepared by coevaporating Ti and C_{60} onto moderately heated substrates (∼100 °C) in an ultrahigh vacuum system. The Ti_xC_{60} films were all amorphous according to X-ray diffraction and exhibited a gray, metallic luster different from the brown color of pristine C_{60}. The compound also appeared to be metallic or semiconducting as no charging was observed in X-ray photoelectron spectroscopy (XPS) in contrast to analyses of pure C_{60}. XPS of the films showed a maximum titanium content of about 5.3−5.5 at. % ($Ti_{\sim 3.5}C_{60}$). For higher titanium contents, carbide formation was observed. The XPS analyses also showed binding energy shifts and line broadening effects consistent with the formation of chemical bonds between Ti and C_{60}. Raman spectroscopy showed a softening of the $A_g(2)$ mode upon Ti incorporation (−4 cm^{-1}/Ti atom) which is consistent with a partial charge transfer from Ti to C_{60}. The Ti_xC_{60} films oxidized immediately upon air exposure. However, XPS and Raman spectroscopy show persistent differences from pristine C_{60} which might indicate that another phase, $Ti_xO_yC_{60}$, is formed upon oxidation.

1. Introduction

C_{60} is a unique molecule insofar as it lends itself to various kinds of doping, thereby forming new solid-state compounds. There are at least three possible types of doping: *endohedral* (dopant inside the C_{60} shell), *substitutional* (part of the shell), or *exohedral* (between the shells). The latter is by far the most extensively studied, presumably due to the early discovery of superconductivity in K_3C_{60}.[1] However, mainly intercalation compounds with the alkali and alkaline-earth metals have been synthesized so far. Only a few reports claiming the existence of fullerides with transition metals are known to the authors. Zhao et al. observed new air-sensitive IR bands for C_{60} doped with Au, In, and Sn which they assign to a fulleride compound.[2] Byszewski et al. reported a thermally unstable Fe_2C_{60} compound which crystallizes in a monoclinic lattice, however, with the reservation that the iron ions may have entered either exohedral or endohedral positions.[3] In addition, new fullerides based on rare-earth metals (Eu, Sm) have recently been synthesized.[4,5]

There are many papers which discuss the thermodynamic instability of transition-metal fullerides. Wertheim et al. present a simple formulation taking into account the LUMO energy of C_{60} as well as the work function and the cohesive energy of the metal.[6] The result of this analysis is that only alkali metals, alkaline-earth metals, and mercury are energetically favorable candidates for intercalation. Wang et al. developed a more complete model by using a thermodynamic Born−Haber cycle that included the cohesive energy of the ionic A_xC_{60} fulleride, and they predicted that alkali and alkaline-earth metals should form stable compounds.[7] Today most authors seem to agree that the fundamental limitation to intercalation of transition

(1) Hebard, A. F.; Rosseinsky, M. J.; Haddon, R. C.; Murphy, D. W.; Glarum, S. H.; Palstra, T. T. M.; Ramirez, A. P.; Kortan, A. R. *Nature* **1991**, *350*, 600.
(2) Zhao, W.; Li, Y.; Chen, L.; Liu, Z.; Huang, Y.; Zhao, Z. *Solid State Commun.* **1994**, *92*, 313.
(3) Ginwalla, A. S.; Balch, A. L.; Kauzlarich, S. M.; Irons, S. H.; Klavins, P.; Shelton, R. N. *Chem. Mater.* **1997**, *9*, 278.
(4) Zhao, W.; Tang, J.; Falster, A. U.; Simmons, Jr., W. B.; Sweany, R. L. *J. Alloys Compd.* **1997**, *249*, 242.
(5) Byszewski, P.; Kowalska, E.; Diduszko, R. *J. Therm. Anal.* **1995**, *45*, 1205.
(6) Wertheim, G. K.; Buchanan, D. N. E. *Solid State Commun.* **1993**, *88*, 97.
(7) Wang, Y.; Tománek, D.; Bertsch, G. F.; Ruoff, R. S. *Phys. Rev. B.* **1993**, *47*, 6711.

S0897-4756(97)00787-4 CCC: $15.00
Published on Web 04/03/1998

metals lies in the high cohesive energy of the metals. This means that the formation of the two-phase system Me(s) + C_{60}(s) is thermodynamically more favorable than the formation of a Me_xC_{60} compound (Me = a transition metal). Nevertheless, it must be pointed out that this fact does not rule out the existence of metastable Me_xC_{60} compounds. Such compounds can, like diamond compared to graphite, not only be synthesized but also exhibit a high degree of stability.

It should be noted that the models described above are based on the hypothesis that the intercalated metal is completely ionized in the fulleride. We think that it is worthwhile to also consider the possibility that transition metals can enter coordination compounds with an orbital overlap between d-orbitals of the transition metal and π-orbitals in C_{60} (i.e. covalent-type bonding). In fact, a number of theoretical and experimental studies have shown that such orbital interactions can exist.[8−13] For example, a Pd_xC_{60} compound with a polymer-like structure has been synthesized.[8,9] Several experimental observations on covalent-like C_{60}−metal interactions have also been reported from studies of, for example, monolayer Me atoms on C_{60} or vice versa. It is conceivable that such interactions also could occur in the bulk and that covalent Me_xC_{60} compounds may be possible to synthesize for a number of transition metals.

It is likely that good candidates for the formation of covalent transition-metal fullerides may be found among metals belonging to group IV to VI in the periodic table since they are known to form fairly strong covalent bonds toward carbon. In fact, electron spectroscopy studies of adsorbed metals on C_{60} surfaces by Ohno et al. have shown that Ti overlayers on C_{60} surfaces behave quite differently from other metals.[14] No metal clustering or carbide formation occurred for Ti coverages lower than ∼5 Å. This behavior was ascribed to a hybridization between metal d- and fullerene p-orbitals. Consequently, we suggest that Ti may also be a good candidate for bulk fullerides.

The interaction between thin layers of Ti and C_{60} has recently been studied by Wang and Wang.[15] They were unable to observe any formation of a Ti_xC_{60} compound but found an indication of a solid-state amorphization to a carbide phase at the metal−C_{60} interface. However, it is quite clear that the formation of a fulleride by annealing of thin Ti/C_{60} films requires relatively high activation energies for Ti−Ti bond breaking. A better approach may therefore be a coevaporation process where Ti and C_{60} are introduced to the surface of the growing material at very low fluxes and moderate substrate temperatures, thereby minimizing the effect of the high cohesive energy of the metal. We have recently used this technique and demonstrated that Ti atoms react strongly with C_{60} at low temperatures to form TiC.[16] The objective of the present study is to investigate the feasibility of using a coevaporation process also to synthesize titanium fullerides.

2. Experimental Section

Thin films of Ti_xC_{60} were deposited by coevaporation of C_{60} and Ti in ultrahigh vacuum (UHV). The evaporation setup consists of a resistively heated Knudsen cell for C_{60} (MER Corp., 99.95%) and an electron beam evaporator for Ti (Goodfellow, 99.99%). The individual fluxes were controlled by cell temperature and emission current, respectively. The substrates (Al_2O_3, SiO_2, Si) were mounted on a graphite filament heater situated approximately 10 cm from the evaporators. The base pressure in the growth chamber was 2×10^{-9} Torr but increased as high as 2×10^{-8} Torr during deposition. The substrate temperature was kept as low as possible (approximately 100 °C) to hinder Ti migration and clustering. The as-deposited films were transferred in vacuo to an X-ray photoelectron spectrometer for chemical analysis and measurement of the atomic composition of the fullerides. The sensitivity factors used in the calculation of the atomic concentration of Ti and C were obtained from analysis of a titanium carbide standard with known composition. The binding energy scale was calibrated by setting the C1s peak for a graphite sample at 284.7 eV[17] and the Ti2$p_{3/2}$ peak for pure Ti at 453.8 eV.[18] Deposition was started and terminated by operating individual shutters for Ti and C_{60}, thereby avoiding compositional gradients due to undefined fluxes at the beginning and end of deposition. X-ray photoelectron spectroscopy (XPS) with intermittent Ar^+ ion sputtering of a Ti_1C_{60} film resulted in a depth profile with no significant variations in Ti content. Films with thicknesses of approximately 600 Å were deposited in 1 h. These films were extremely air-sensitive and degraded rapidly by oxidation upon exposure to air. This problem was solved by transferring the films back to the deposition chamber following XPS analysis and capping the surface with a thin film of pure titanium, thereby forming an oxygen diffusion barrier sufficient to enable ex situ analyses within at least a few weeks. However, great care had to be taken to avoid any defects (e.g. pinholes) in the cap layer as will be discussed below. The capping method was used to characterize the film with X-ray diffraction (Siemens D5000 diffractometer with Cu Kα radiation) and Raman spectroscopy. Raman spectra with a resolution of 2 cm^{-1} were recorded at room temperature (295 K) using a Renishaw System 1000 spectrometer equipped with an argon ion laser (514.5 nm) and an Olympus microscope. Raman analyses on Ti-capped films were carried out from the backside, through the Al_2O_3 or SiO_2 substrates (0.6 mm thick) using a backscattering geometry. In the initial attempts, scattered light from the substrate dominated the Raman spectra. Therefore, a confocal technique combined with a long working distance objective (8 mm) was used, thereby reducing the lateral resolution to ∼2 μm. On the oxidized samples, Raman analyses were carried out by a nonconfocal setup from the front side, using a different spectrometer equipped with a diode laser (780 nm).

3. Results and Discussion

Initial experiments showed that the coevaporation of Ti and C_{60} produces films which are quite different from

(8) Nagashima, H.; Nakaoka, A.; Saito, Y.; Kato, M.; Kawanishi, T.; Itoh, K. *J. Chem. Soc., Chem. Commun.* **1992**, 377.
(9) Cowley, J. M.; Liu, M.-Q.; Ramakrishna, B. L.; Peace, T. S.; Wertsching, A. K.; Pena, M. R. *Carbon* **1994**, *32*, 746.
(10) Maxwell, A. J.; Brühwiler, P. A.; Nilsson, A.; Mårtensson, N.; Rudolf, P. *Phys. Rev. B* **1994**, *49*, 10717.
(11) Maxwell, A. J.; Brühwiler, P. A.; Andersson, S.; Arvanitis, D.; Hernnäs, B.; Karis, O.; Mancini, D. C.; Mårtensson, N.; Gray, S. M.; Johansson, M. K.-J.; Johansson, L. S. O. *Phys. Rev. B* **1995**, *52*, R5546.
(12) Lichtenberg, D. L.; Wright, L. L.; Gruhn, N. E.; Rempe, M. E. *J. Organomet. Chem.* **1994**, *478*, 213.
(13) López, J. A.; Mealli, C. J. *J. Organomet. Chem.* **1994**, *478*, 161.
(14) Ohno, T. R.; Chen, Y.; Harvey, S. E.; Kroll, G. H.; Benning, P. J.; Weaver, J. H. *Phys. Rev. B.* **1993**, *47*, 2389.
(15) Wang. W. H.; Wang, W. K. *J. Appl. Phys.* **1996**, *79*, 149.
(16) Norin, L.; McGinnis, S.; Jansson, U.; Carlsson, J.-O. *J. Vac. Sci. Technol. A* **1997**, *15*, 3082.
(17) Belton, D. N.; Schmieg, S. J. *J. Vac. Sci. Technol. A* **1990**, *8*, 2353.
(18) Wagner, C. D., Riggs, W. M., Davis, L. E., Moulder, J. F., Muilenberg, G. E., Eds. *Handbook of X-ray Photoelectron Spectroscopy*; Perkin-Elmer Corporation, Physical Electronics Division: Eden Prairie, Minnesota, 1979.

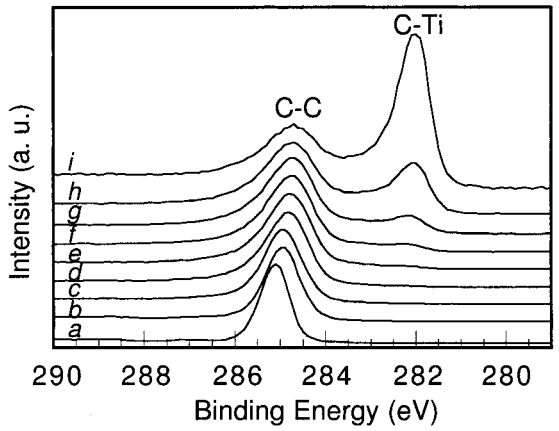

Figure 1. XPS C1s spectra for films with different Ti contents, obtained by coevaporating Ti and C_{60} onto a substrate heated to 100 °C. The Ti concentrations (atomic percent) from bottom to top are (a) 0, (b) 2.3, (c) 3.6, (d) 5.5, (e) 8.4, (f) 12, (g) 19, (h) 31, (i) 46.

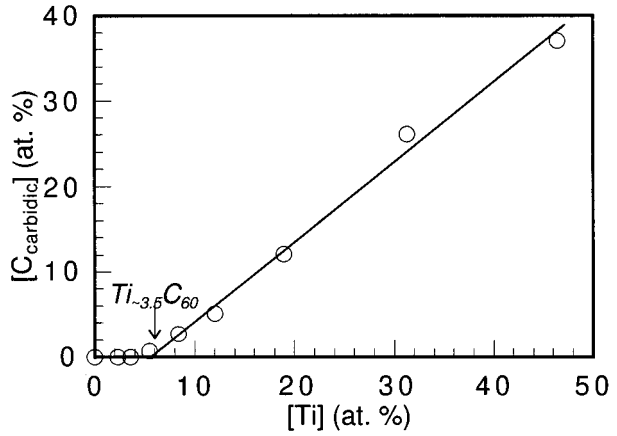

Figure 2. Carbidic carbon content vs Ti content (overall concentrations in at. %) obtained from XPS analysis of films deposited with different Ti/C_{60} ratios at a substrate temperature of 100 °C.

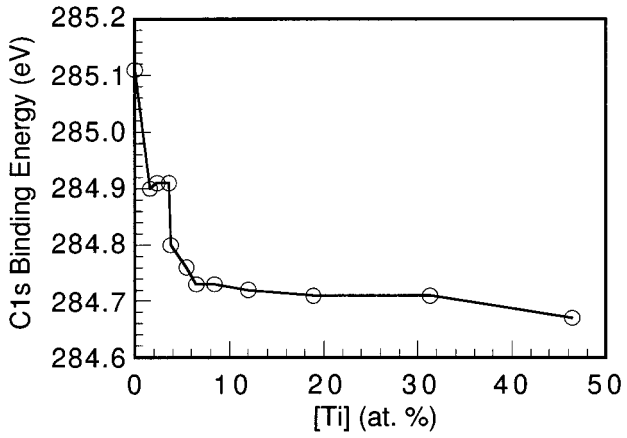

Figure 3. XPS C1s binding energy vs Ti content.

pristine C_{60}. For example, as-deposited Ti_xC_{60} films appear dark gray with a clear metallic luster compared to the brown-colored C_{60} films. Furthermore, Ti_xC_{60} films deposited on insulating substrates did not charge during XPS analysis in contrast to pure C_{60} films. These results suggest that the coevaporation of Ti and C_{60} leads to the formation of a new type of compound with metallic or semiconducting properties.

All attempts to characterize the Ti_xC_{60} films ex situ without a capping layer failed. This was due to a fast oxidation, which could be seen as a change in color from a gray, metallic luster to a brownish nuance similar to pristine C_{60}. XPS analysis confirmed that films exposed to air were oxidized (oxygen content ~5−10 at. %). Furthermore, a substantial charging in the XPS analysis suggested that the conductive properties of the films also had changed. This was further confirmed by four-probe resistivity measurements which showed that the air-exposed films were insulating. Consequently, all studies of the assumed Ti_xC_{60} compound had to be carried out in situ on as-deposited films or by using a capping procedure where the fulleride was covered by a thin layer (~200 Å) of metallic titanium.

X-ray diffraction of capped Ti_xC_{60} ($x \approx 1-3$) deposited at 100 °C showed no peaks, suggesting that these films are amorphous. It is plausible that the crystallinity of the films can be improved by an increase in deposition temperature. However, all attempts to deposit Ti_xC_{60} films at substrate temperatures of 200 and 300 °C failed since the Ti content in the films could not be reduced below approximately 15−20% regardless of the decrease in Ti flux. This Ti content is far too high for fulleride formation, as will be discussed in the next section. The reason for this behavior is currently unknown and further studies are required to gain a complete understanding of the influence of temperature on the synthesis of the Ti_xC_{60} films.

3.1. XPS Analysis of the Ti_xC_{60} Films. In situ XPS studies of the deposited films confirmed that titanium interacts strongly with C_{60}. Figure 1 shows a series of C1s XPS spectra from films obtained by coevaporation of Ti and C_{60} at 100 °C. As can be seen in this figure, high Ti/C_{60} flux ratios result in two C1s peaks at approximately 282.0 and 284.8 eV, which can be attributed to carbon bonded in TiC and to carbon bonded in a C_{60}-type compound, respectively. The amount of carbidic carbon (assessed by curve fitting the C1s peaks at 282.0 and 284.8 eV, respectively) was directly proportional to the Ti concentration in the film (Figure 2). The observations clearly show that Ti, at high concentrations, can break the cage structure of C_{60} at temperatures as low as 100 °C. The striking part in Figure 2, however, is that no signs of carbide formation can be seen for low Ti concentrations. Extrapolation of the graph from the linear part shows that no carbide formation occurs until the Ti content exceeds approximately 5.3−5.5 at. % (Ti/C_{60} ≈ 3.5). We interpret this as a phase boundary between titanium carbide and a new Ti_xC_{60} fulleride ($0 < x < 3.5$).

The formation of a new Ti_xC_{60} phase is also supported by a more detailed study of the C1s and Ti2p peaks which show clear chemical shifts. The C1s peak shifts to lower binding energies upon Ti incorporation (Figure 3). As can be seen in this plot, the downshift is initially dependent on the Ti content and decreases from 285.1 (pure C_{60}) to 284.75 eV at 6 at. %, whereupon it levels out at approximately 284.7 eV. It could be argued that the shift is caused by changes in charging when Ti is added to the growing film. However, we have not observed any significant charging effects in thin C_{60} films deposited on conducting substrates. Furthermore, the Ti2p peaks from the Ti_xC_{60} films are also clearly shifted, but in the opposite direction, toward higher

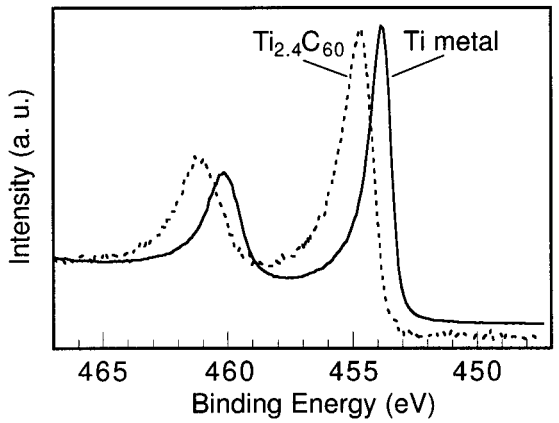

Figure 4. XPS Ti2p spectra showing a chemical shift of 0.84 eV for $Ti_{2.4}C_{60}$ compared to pure Ti.

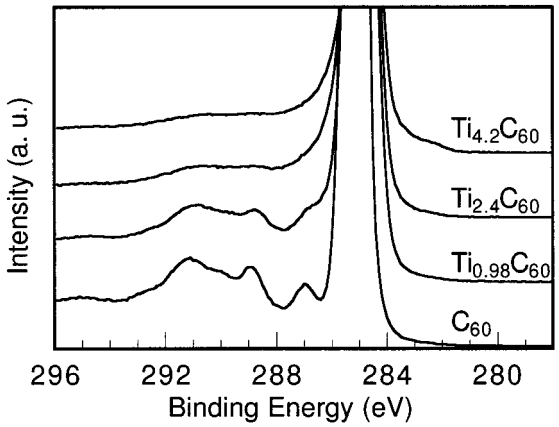

Figure 5. XPS C1s derived satellite structures for C_{60} and Ti_xC_{60} (x = 0.98, 2.4, 4.2).

binding energies (~0.8 eV) compared to pure titanium. The shift is more or less independent of the Ti content (see Figure 4). The results in Figures 3 and 4 are consistent with the formation of a new compound with a charge transfer from Ti to C_{60}. A rough estimate of the Ti charge state was obtained by plotting the chemical shift versus Ti oxidation number for six different titanium oxides. Fitting a straight line to this plot yields a slope of ~1.2 eV shift per Ti oxidation number, which results in a Ti charge state of 0.8/1.2 ≈ 0.66 when applied to the Ti fullerides.

Further detailed analyses of the C1s peaks originating from pure C_{60} and from Ti_xC_{60} films also clearly show a broadening and attenuation of the shake-up satellites above the C1s peak (see Figure 5). A pure C_{60} film exhibits a number of satellites at energies above the C1s main peak (bottom, Figure 5). The first satellite above the main peak is identified by excitations across the HOMO−LUMO gap of 1.9 eV, while the peaks at higher binding energies are attributed to dipole excitations.[19] As can be seen in Figure 5, the addition of Ti to the films broadens and reduces the intensity of the shake-up peaks. For a $Ti_{0.98}C_{60}$ film, the satellites are still present, although broader and with the first satellite grown together with the main peak. For a composition of $Ti_{2.4}C_{60}$, the satellites are no longer discernible. For

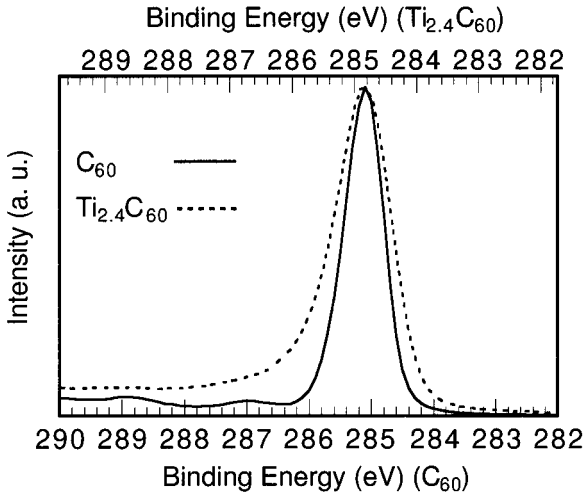

Figure 6. XPS C1s spectra for $Ti_{2.4}C_{60}$ and C_{60}. The spectra have been overlaid for easier comparison of peak shapes.

the highest Ti level in Figure 5 ($Ti_{4.2}C_{60}$) one can also note a weak shoulder to the right of the C1s peak. This indicates that parts of the C_{60} molecule have decomposed to form titanium carbide. The satellite-broadening effect has previously been observed for C_{60} chemisorbed on metal surfaces and can be assigned to a hybridization between Ti and both the occupied and unoccupied molecular orbitals of C_{60}.[10] Furthermore, the addition of Ti also broadens the main C1s peak (Figure 6). This peak has a fwhm of about 0.75 eV in pure C_{60} compared to 1.1 eV in $Ti_{2.4}C_{60}$. The peaks also show an asymmetry toward higher binding energies. This effect has also been observed during chemisorption of C_{60} on metals and can be assigned to two factors: the formation of inequivalent carbon sites and the formation of electron−hole pairs in a partly filled band.[10] We cannot determine the contribution of these factors to the line width, but it is clear that both mechanisms are consistent with the conclusion that a Ti_xC_{60} compound is formed in our experiments.

3.2. Raman Spectroscopy of the Ti_xC_{60} Films. Ex situ Raman spectroscopy on Ti_xC_{60} films provided a further support for compound formation. The analyses were carried out on capped films deposited on Al_2O_3 or SiO_2 substrates by probing the film, through the substrate, from the backside. Excitation by a 780 nm diode laser, with a confocal setup, was initially used for the analysis. This wavelength was used to avoid the photopolymerization known to occur for pristine C_{60} when using a 514.5 nm argon ion laser.[20] In contrast to pristine (and Ti-capped) C_{60} layers, the Ti_xC_{60} films were highly reflective at this wavelength and, therefore, more or less impossible to analyze. This observation supports the previous conclusion that a metallic or semiconducting Ti_xC_{60} compound is formed. It was possible, however, to obtain Raman spectra from the fulleride film by using a 514.5 nm argon ion laser. In this case, a low power density (<50 mW/cm^2) was used to avoid polymerization in pristine C_{60}, as indicated by the position of the $A_g(2)$ peak.

The spectra from a series of fullerides with compositions ranging from $Ti_{0.98}C_{60}$ to $Ti_{5.6}C_{60}$ showed a clear

(19) Weaver, J. H.; Martins, J. L.; Komeda, T.; Chen, Y.; Ohno, T. R.; Kroll, G. H.; Troullier, N.; Haufler, R. E.; Smalley, R. E. *Phys. Rev. Lett.* **1991**, *66*, 1741.

(20) Rao, M.; Zhou, P.; Wang, K. A.; Hager, G. T.; Holden, J. M.; Wang, Y.; Lee, W. T.; Bi, X.-X.; Eklund, P. C.; Cornett, D. S.; Duncan, M. A.; Amster, I. J. *Science* **1993**, *259*, 955.

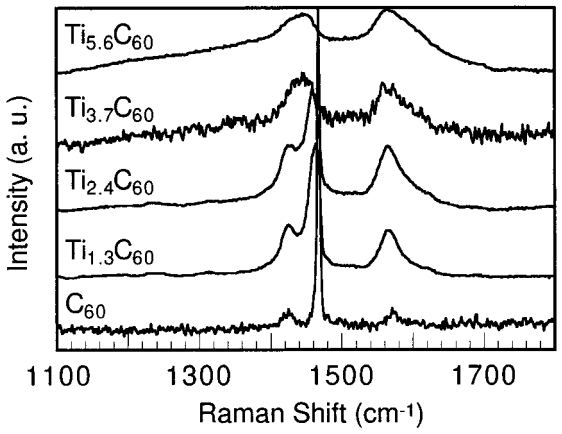

Figure 7. Raman spectra of Ti-capped Ti_xC_{60} films (x = 1.3, 2.4, 3.7, 5.6). A spectrum of pristine C_{60} (bottom) is also shown for comparison.

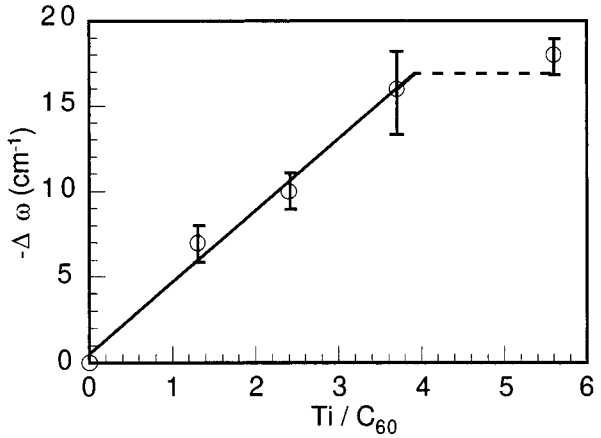

Figure 8. Dependence of the frequency of the $A_g(2)$ mode on the number of Ti per C_{60}.

downshift of the $A_g(2)$ peak (see Figure 7). This peak is found at 1469 cm^{-1} for pure C_{60} but is shifted to about 1453 cm^{-1} for $Ti_{3.7}C_{60}$. For a composition of $Ti_{5.6}C_{60}$ the position of the $A_g(2)$ peak is about the same as for $Ti_{3.7}C_{60}$. This is in good agreement with the XPS data that suggested a maximum solubility of approximately 3−4 Ti atoms per C_{60}. Up to that point, the shift is clearly proportional to the Ti concentration, and it is reasonable to postulate a linear relationship between shift and Ti content (Figure 8). The shift can be estimated to be approximately −4 cm^{-1} per Ti atom and is consistent with a charge transfer from Ti to the antibonding π-orbitals in C_{60}. This can be compared with an $A_g(2)$ downshift of approximately 6 cm^{-1} for each metal atom in the alkali-metal fullerides.[21] The results suggest a lower extent of charge transfer in Ti_xC_{60} compared to that in the alkali-metal fullerides. With 6 cm^{-1} downshift per accepted electron, the average electron transfer from each Ti atom could be estimated to $^4/_6 \times 1 \approx 0.66$, which is in good agreement with XPS analysis. Similarly, the valence state of the C_{60} molecule in each compound can be estimated as −1.2 ($Ti_{1.3}C_{60}$), −1.7 ($Ti_{2.4}C_{60}$), −2.7 ($Ti_{3.7}C_{60}$), and −3.0 ($Ti_{5.6}C_{60}$).

A more detailed study of the Raman spectra in Figure 7 also shows two other effects: line broadening of the peaks and a relative decrease of the intensity of the $A_g(2)$ mode at 1469 cm^{-1} compared to the intensities of the H_g modes at about 1425 and 1570 cm^{-1}, respectively. Line broadening of Raman peaks has previously been observed also in alkali metal fullerides and has been attributed to enhanced electron−phonon coupling.[22] However, it should be noted that the Ti_xC_{60} films in our study are amorphous, which means that a distribution of bond angles, bond lengths, and coordination numbers between Ti and C_{60} are likely to prevail within the material. The disorder may, through Ti−C_{60} bonds, even result in a distortion of the original C_{60} cage and give rise to the line broadening observed in Figure 7. Although this effect to some extent can reduce the intensity of the prominent $A_g(2)$ feature, the complete role of the Ti doping versus the mode intensities remains unclear.

3.3. Oxidation of Ti_xC_{60}. As mentioned above, the Ti_xC_{60} films exposed to air oxidize quickly with a subsequent change in color from a dark metallic luster to a brownish, transparent film similar to pure C_{60}. The oxidized films are also insulating according to the four-probe resistivity measurements. This was confirmed by XPS analysis of films deposited on insulating sapphire substrates which showed severe charging effects after air-exposure but not for the as-deposited films.

The XPS analysis showed that the oxygen content in the oxidized films was approximately 5−10 at. %. A more detailed study of the XPS spectra showed that the C1s peak is completely unaffected by oxidation, i.e. binding energy and broadening of the C1s main peak and shake-up satellites are identical in oxidized and unoxidized Ti_xC_{60} films. This clearly suggests that the chemical nature of the C_{60} molecule is unaffected by oxidation. In contrast, the $Ti2p_{3/2}$ and $Ti2p_{1/2}$ peaks are shifted about 4 eV to binding energies of 458.8 and 466.1 eV, respectively. These values correspond to the Ti2p binding energies in TiO_2 and suggest that Ti−O bonds have been formed that are similar to those found in TiO_2. However, it is unlikely that the oxidation leads to a simple decomposition of the titanium fulleride into C_{60} and TiO_2 since the C1s peak clearly shows all features typical for Ti_xC_{60} as described above. Furthermore, immersion of an air-exposed $Ti_{3.0}C_{60}$ film in toluene resulted in no observable dissolution in several days, in contrast to pure C_{60} films which dissolve completely within a few seconds. Consequently, we conclude that the oxidation of Ti_xC_{60} results in the formation of a new compound, $Ti_xO_yC_{60}$. The nature of the chemical bonds between C_{60}, O, and Ti in this compound cannot be determined from the present data. However, we are currently carrying out soft X-ray spectroscopy analysis of this material, and the results will be published elsewhere.

The color change upon oxidation described above can be used to study the oxidation process visually in real time by a simple experiment in which a Ti_xC_{60} film protected by a thin film of titanium was locally damaged in the cap layer while viewing the film from the backside (through the substrate) under a light optical microscope. Immediately following the scratching, a distinct lighter front of oxidized Ti_xC_{60} emerged out from the groove

(21) Dresselhaus, M. S.; Dresselhaus, G.; Eklund, P. C. *J. Raman Spectrosc.* **1996**, *27*, 351.

(22) Mitch, M. G.; Lannin, J. S. *Phys. Rev. B* **1995**, *51*, 6784.

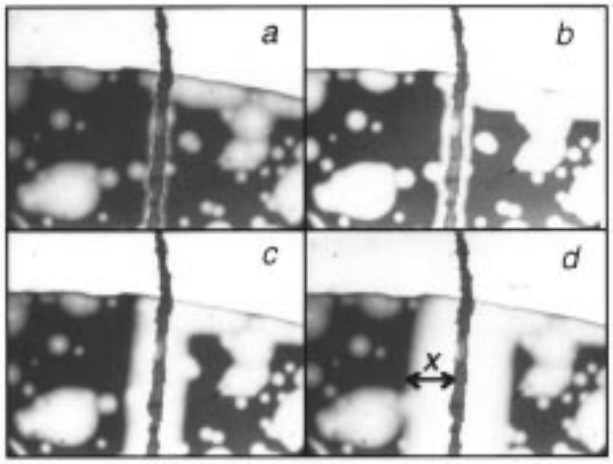

Figure 9. Light optical microscope images of a Ti-capped $Ti_{3.4}C_{60}$ film as viewed through the sapphire substrate. The pictures show part of a $Ti_{3.4}C_{60}$ film with a diameter of 6 mm (lower dark region), capped with Ti extending over the edges of the film (upper light region). The light spots in the film correspond to oxidized material as a result of an unsuccessful capping procedure (each spot was found to have a pinhole in its center). The dark vertical groove in the center was created to penetrate the cap layer at $t = 0$ min. Oxidation is seen as a light band surrounding the groove, here shown for $t =$ (a) 2, (b) 4, (c) 22, and (d) 92 min.

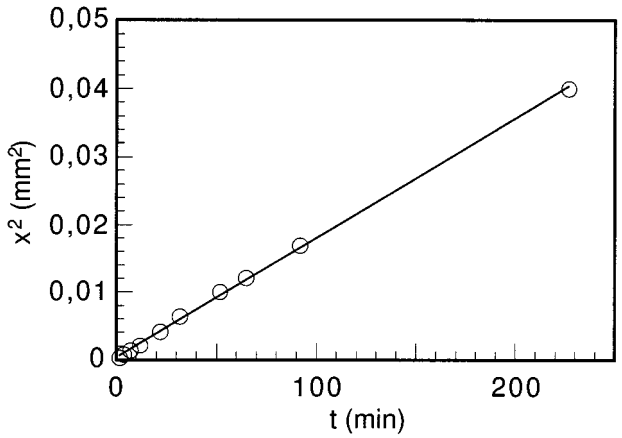

Figure 10. x^2 vs t, where x is the distance marked in Figure 9d and t is the time after penetrating the cap layer.

(Figure 9). By measuring the distance, x (m), between the light front and the created groove at different times, t (s), and plotting x^2 versus t, a linear relation is obtained that is indicative of a diffusion-controlled process (Figure 10). From the slope of this line (1.8×10^{-4} mm^2/min $= 2.9 \times 10^{-12}$ m^2/s), it can be calculated that a 600 Å thick Ti_xC_{60} film will oxidize from surface to substrate in ~1 ms, if exposed uncapped in air. It is not a trivial task to calculate the diffusion coefficient, D, for oxygen in Ti_xC_{60} from the type of curve shown in Figure 10. However, a rough estimate of D can be obtained from the slope of the curve by assuming Fick's 1st law to be applicable, i.e. $x^2 = -2D\Delta ct$ and by assuming that the solid solubility of oxygen in Ti_xC_{60} is complete with a constant concentration of 10 at. % ($Ti_{3.4}O_{6.8}C_{60}$) at the groove−air interface. Furthermore, assume that the oxygen concentration is approximately zero at the light/dark border, giving $\Delta c \approx -10$ at. %. This gives an approximate value of $D \approx 1.5 \times 10^{-11}$ m^2/s if the slope K in Figure 10 is given by $K = -2D\Delta c$ ($K = 2.9 \times 10^{-12}$ m^2/s). This rather high value for solid-state diffusion at room temperature can be compared with reported values for O_2 diffusion in bulk C_{60} of D(300 K) $\approx 1.7 \times 10^{-21}$ to 1.7×10^{-19} m^2/s obtained from semiempirical calculations.[23]

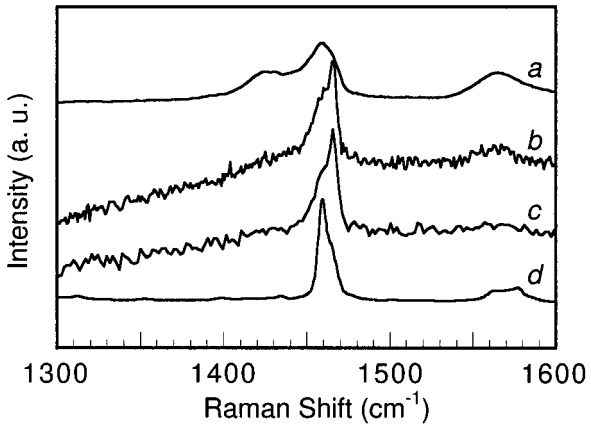

Figure 11. Raman spectra of (a) nonoxidized $Ti_{2.4}C_{60}$, (b) oxidized $Ti_{2.7}C_{60}$, (c) oxidized $Ti_{1.1}C_{60}$, and (d) pressure-polymerized C_{60}.

The change in electronic properties of the Ti_xC_{60} films upon oxidation was also seen in Raman spectroscopy: In contrast to the capped Ti_xC_{60} films, the oxidized Ti_xC_{60} films were easily analyzed with near-infrared excitation (780 nm) to yield spectra which were completely different from those obtained for capped films. As a result of oxidation, most of the H_g modes became very weak and the region around the "pentagonal pinch", $A_g(2)$, mode changed dramatically in character. In Figure 11 this region is shown for a capped $Ti_{2.4}C_{60}$ (a) and two oxidized (b, c) films. Even though the molecular structure of the new $Ti_xO_yC_{60}$ compounds is unknown, we note that in this region there is an overall similarity with polymerized C_{60}. The strong $A_g(2)$ mode at 1469 cm^{-1} is sensitive to the degree of polymerization since the frequency downshifts to 1459 cm^{-1} in photopolymerized samples[24] as well in pressure-treated samples.[25] For comparison a partly pressure polymerized C_{60} film (1 GPa, 500 K) is therefore shown in Figure 11d. The observed similarity may be accidental, but we note that polymerization of C_{60} as a result of doping has previously been observed in AC_{60} compounds for A = K, Rb, and Cs.[26] The Raman results on $Ti_xO_yC_{60}$ compounds may therefore be related to linkages between the C_{60} molecules, but further work on the new compounds is needed to address this issue.

4. Conclusions

By coevaporating C_{60} and Ti on a substrate heated to approximately 100 °C, a new amorphous Ti_xC_{60} phase is formed, which can include up to 3−4 Ti atoms per C_{60}. Higher Ti concentrations lead to a decomposition of the C_{60} molecules and the formation of TiC. We believe that the success of coevaporation compared to

(23) Halac, E.; Burgos, E.; Bonadeo, H. *Phys. Rev. B* **1995**, *52*, 4764.
(24) Eklund, P. C.; Zhou, P.; Wang, K. A.; Dresselhaus, G.; Dresselhaus, M. S. *J. Phys. Chem. Solids* **1992**, *53*, 1391.
(25) Wågberg, T.; Persson, P.-A.; Sundqvist, B.; Jacobsson, P. *Appl. Phys. A* **1997**, *64*, 223.
(26) Winter, J.; Kuzmany, H. *Solid State Commun.* **1992**, *53*, 1321.

other techniques (e.g. annealing of Ti/C_{60} layers) is due to the fact that the effect of the cohesive energy of the metal is minimized. Furthermore, the sensitivity of the Ti_xC_{60} compound toward oxidation suggests that very good vacuum conditions (i.e. UHV) are required for a successful synthesis.

XPS and Raman spectroscopy of the Ti_xC_{60} films show peak shifts and other features which are consistent with a chemical bonding between Ti and C_{60}. The nature of the bonding within this compound cannot be determined from our results. However, we believe that the Ti−C bonding includes a strong covalent contribution. This is supported by the fact that the Raman spectra suggest a lower extent of charge transfer in the Ti_xC_{60} films compared to corresponding alkali-metal fullerides. Our data give no information about how C_{60} coordinates Ti. However, theoretical studies have shown that for some transition metals, the energetically most favored bonding position is directly above the fusion of two six-membered rings (η^2 coordination).[12,13] Studies of many organometallic complexes have shown that this position indeed is a favorable site where the C_{60} molecule prefers to coordinate as an electron-deficient η^2-alkene-like fragment.[27] This type of bonding has also been proposed for Pd_xC_{60} where each Pd atom can bond to two or more C_{60} molecules thereby producing unbranched or branched polymer chains.[8,9] It is possible that the Ti_xC_{60} compound described in our paper exhibits a similar type of bonding. Further studies, however, are required to elucidate the details in this matter.

The Ti_xC_{60} films are extremely air-sensitive and have to be handled in UHV to avoid oxidation. XPS and Raman spectroscopy suggest that the Ti_xC_{60} compound does not recover to normal C_{60} upon oxidation but forms another compound, $Ti_xO_yC_{60}$. This is also supported by the fact that the oxidized Ti_xC_{60} films are insoluble in toluene. No physical properties have yet been obtained for the nonoxidized Ti_xC_{60} compound because of the difficulties in handling this material in air. However, our results suggest that Ti_xC_{60} is semiconducting or metallic at room temperature, and attempts to measure the electric conductivity will be carried out soon.

Acknowledgment. The Swedish Research Council for Engineering Sciences (TFR), the Swedish Natural Science Research Council (NFR), and the Ångström Consortium are acknowledged for financial support.

CM9707871

(27) Green, M. L. H. *Pure Appl. Chem*. **1995**, *67*, 249.